ARBITRARY PULSE SHAPING USING ACCELERATED INTERFACES

Amir Bahrami
Department of Electrical Engineering
KU Leuven
Leuven, 3001
abahrami@esat.kuleuven.be

Klaas De Kinder
Department of Electrical Engineering
KU Leuven
Leuven, 3001
klaas.dekinder@kuleuven.be

Department of Electrical Engineering
KU Leuven
Leuven, 3001
christophe.caloz@kuleuven.be

June 12, 2025

ABSTRACT

We propose a novel method for arbitrary pulse shaping based on nonuniform Doppler shifts induced by an accelerated perfect electric conductor (PEC) interface. Unlike conventional pulse shaping techniques, which rely on spectral filtering or nonlinear effects, our approach leverages the controlled motion of an interface to directly reshape the temporal envelope of an optical pulse. We begin by deriving the exact scattering relations for an arbitrarily moving PEC interface and solving the inverse problem to determine the required trajectory that transforms a given input pulse into a desired waveform. The proposed method is validated through illustrative examples, demonstrating its ability to reshape Gaussian pulses into various target profiles, including modulated, rectangular and asymmetric waveforms. Additionally, we confirm our theoretical predictions via finite-difference time-domain simulations.

1 Introduction

Pulse shaping is the process of modifying the temporal or spectral characteristics of optical pulses to achieve specific profiles [1]. Optical pulses are fundamental tools in modern optics and photonics; making pulse shaping pivotal in applications such as chirped pulse amplification [2], dispersion compensation [3], nonlinear optical processing [4, 5], short-pulse generation [6], amplifier phase control [7], bandpass filtering [8], quantum manipulations [9] and analog signal processing [10]. Additionally, optical pulses are widely employed in material engineering, micromachining [11, 12] and the control of quantum dynamics [13]. A primary method for pulse shaping involves manipulating its spectral components [14]. This is typically accomplished using diffraction gratings to perform a Fourier transform of the pulse, followed by spectral filtering via masks. Other implementations include acousto-optic tunable filters [15], liquid crystal modulators [16], moving [17] and deformable mirrors [18]. For low-frequency applications, pulse shaping is performed by direct temporal manipulation, such as amplitude modulation, pulse stacking [19] and nonlinear effects [1].

Existing pulse shaping techniques, while effective in various applications, all come with inherent limitations that restrict their flexibility and efficiency. For example, spatial light modulators enable flexible control of arbitrary pulse shapes but are constrained by resolution and response time [20]. Acousto-optic modulators facilitate dynamic and programmable shaping but suffer from signal degradation due to acoustic interactions and limited bandwidth [21, 22]. Pulse stacking, for example, can lead to temporal jitter and signal degradation, whereas nonlinear pulse shaping generate unwanted harmonics in the output. These challenges highlight the need for an alternative approach that can offer greater control and efficiency in reshaping pulses. One way to overcome these constraints is to move beyond conventional spectral filtering and nonlinear interactions and instead manipulate wave propagation through dynamic, space-time modulated media. A related general approach to achieving this lies in Generalized Space-Time Engineered Modulation

(GSTEM) systems [23], which, by allowing material properties to vary in both space and time, can enable novel pulse transformations that are inaccessible with traditional techniques.

GSTEMs, also referred to as space-time modulation metamaterials, are advanced media formed by modulating a host material's properties (e.g., refractive index) in both space and time [24, 25, 23]. These modulations, typically induced by external drives such as electronic, optical, acoustic, or mechanical signals [26, 1, 27], can take the form of traveling or standing waves within the constitutive parameters of the medium. Unlike moving-matter systems, GSTEMs involve no net motion of atoms and molecules; instead, they rely on moving perturbations, thereby combining the benefits of moving media with the practicality of stationary platforms. This approach enables diverse phenomena, including Doppler shifting, Fresnel-Fizeau drag, wave compression amplification [28, 29, 30, 31, 32] and analogs of gravitational effects [33, 34]. While the majority of GSTEM research has centered on purely temporal [35] and uniform-velocity modulations, which underpin applications like time reversal [36], beam splitting, photon generation [37] and Doppler shifting [38], accelerated modulations represent a groundbreaking frontier [23, 39]. By extending beyond uniformity, accelerated modulation introduces new physical effects, such as controllable photon emission [40], distributed analog gravity and light bending effects [41] as well as more complex structures such as space-time wedges [42]. Additionally, acceleration introduces a nonuniform Doppler shift due to the varying velocity, nonuniformly altering the spectral composition of the pulse [43, 44].

Here, we leverage nonuniform Doppler shifts generated by wave interactions with a *nonuniformly moving* perfect electric conductor (PEC) interface to achieve precise and highly controllable pulse shaping. To establish the foundation of this technique, we first derive the scattering relations governing the interaction of electromagnetic waves with a PEC interface that undergoes arbitrary nonuniform motion. With these relations in hand, we address the inverse problem by analytically determining the specific trajectory of the interface required to transform an input pulse envelope into a desired output waveform. Finally, to showcase the versatility and effectiveness of the method, we present demonstrations where a Gaussian pulse is reshaped into more intricate waveforms.

The remainder of the paper is organized as follows. First, in Sec. 2, we introduce the concept of pulse shaping using nonuniform Doppler shifts at an arbitrarily moving PEC interface. Then, in Sec 3, we solve the general scattering problem at an arbitrarily moving PEC interface and derive an exact closed form solution for the scattered wave. Next, in Sec. 4, we solve the synthesis problem, determining the required interface trajectory to transform a given input pulse into a desired shape. The analytical framework and key equations are presented. We subsequently demonstrate the method's versatility through examples in Sec. 5, including reshaping Gaussian pulses into symmetric, rectangular, and asymmetric waveforms, with detailed space-time representations. Finally, Sec. 6 concludes the paper by summarizing key findings and discussing potential applications.

2 Concept

Figure 1 illustrates the fundamental concept of pulse shaping using a PEC interface with arbitrary motion. Figures 1(a) and 1(b) demonstrate the scattering behavior at a uniformly moving PEC interface. When the interface is receding, as shown in Fig. 1(a), the pulse undergoes stretching, accompanied by a decrease in amplitude; in contrast, when the interface approaches, as shown in Fig. 1(b), the pulse is compressed, leading to an increase in amplitude [30]. However, the velocity of the interface does not need to be uniform. A more general scenario arises when the interface alternates between receding and approaching motions. For instance, as illustrated in Fig. 1(c), the interface reverses direction at time t_0. In this case, the portion of the pulse that interacts with the approaching interface is compressed and amplified, whereas the portion that interacts with the receding interface is stretched and attenuated. By carefully engineering the trajectory of the moving interface, one can impose arbitrary deformations on the pulse shape. In principle, this technique allows for highly complex transformations, such as morphing the envelope of a cat into that of a camel, as humorously depicted in Fig. 1(d). The ultimate goal of this work is to derive an analytical equation that dictates the trajectory of the interface required to reshape a given pulse into any arbitrary form.

3 Analysis

This section addresses the problem of wave scattering at an arbitrarily moving PEC interface. We assume general traveling waveforms for both the incident and reflected pulses in vacuum, viz.,

$$E_{\mathrm{i}} = \psi_{\mathrm{i}}[z-t]\hat{x}, \quad B_{\mathrm{i}} = \psi_{\mathrm{i}}[z-t]\hat{y} \tag{1a}$$

and

$$E_{\mathrm{r}} = -\psi_{\mathrm{r}}[z+t]\hat{x}, \quad B_{\mathrm{r}} = \psi_{\mathrm{r}}[z+t]\hat{y}, \tag{1b}$$

where we have used natural units ($c = 1$) and where the square brackets, $[\cdot]$, indicate function arguments. Moreover, we describe the motion of the PEC interface by the implicit equation $z = Z[t]$. This assumption allows for arbitrary,

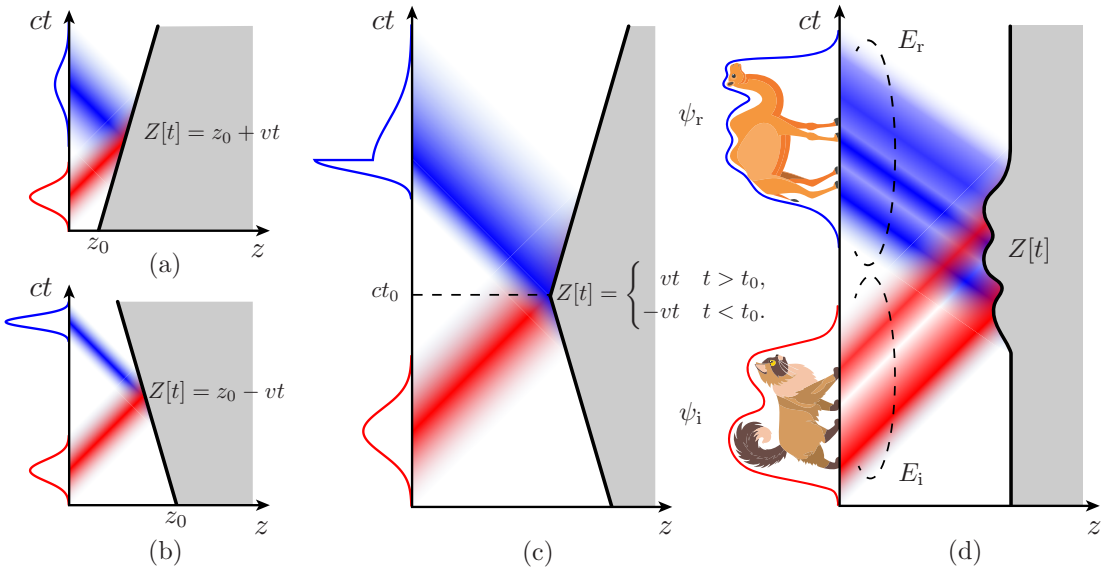

Figure 1: Pulse deformation due to Doppler shift. (a) Pulse expansion (receding interface). (b) Pulse compression (approaching interface). (c) Pulse compansion (receding and approaching interface). (d) Shaping the envelope of a cat into an envelope of a camel via reflection at a moving modulation interface with a judiciously chosen velocity.

time-dependent interface trajectories, providing a general model for analyzing nonuniform motion and its impact on wave scattering.

We now impose the moving boundary conditions for a moving PEC, requiring that the quantity $\mathbf{E} + \mathbf{v} \times \mathbf{B}$ vanishes at the interface (see Supplementary Sec. 1 for detailed derivations), i.e.,

$$\mathbf{E} + \mathbf{v} \times \mathbf{B}\Big|_{z=Z[t]} = (E_\mathrm{i} + E_\mathrm{r}) + Z'[t]\hat{z} \times (B_\mathrm{i} + B_\mathrm{r}) = 0, \tag{2}$$

where the prime denotes the temporal derivative, yielding a velocity. Substituting Eqs. (1) into Eq. (2) gives

$$\psi_\mathrm{r}\left[Z[t] + t\right] = \frac{1 - Z'[t]}{1 + Z'[t]} \psi_\mathrm{i}\left[Z[t] - t\right]. \tag{3}$$

Note that Eq. (3) is valid only at the interface, namely at $z = Z[t]$. In order to determine the reflection profile across *all space-time* as a function of $z + t$, we force the argument of ψ_r to take a traveling waveform, $z + t$, namely we perform the change of variables $Z[t] + t \to z + t$, which yields the final expression for the reflected wave,

$$\psi_\mathrm{r}[z + t] = \frac{1 - Z'[f^{-1}[z + t]]}{1 + Z'[f^{-1}[z + t]]} \psi_\mathrm{i}\left[Z[f^{-1}[z + t]] - f^{-1}[z + t]\right], \tag{4a}$$

where

$$f[t] = Z[t] + t. \tag{4b}$$

Equation (4) is not trivial. To better understand it, let us consider a simple example. Assume a uniform-velocity interface trajectory. Such a trajectory is expressed as $Z[t] = z_0 + vt$ [Fig. 1(a)]. Using Eq. (4b), we find $f[t] = z_0 + (1 + v)t$, whose *inverse function* is $f^{-1}[t] = (1 + v)^{-1}(t - z_0)$. Upon substitution of this last relation in Eq. (4a), we find

$$\psi_\mathrm{r}[z + t] = \frac{1 - v}{1 + v} \psi_\mathrm{i}\left[-\frac{1 - v}{1 + v}(z + t) + \frac{2z_0}{1 + v}\right], \tag{5}$$

as the scattering relation at a uniformly moving PEC interface [45]. It is important to note that, for an accelerated interface, one cannot simply replace v with $v[t]$ in Eq. (5) to obtain Eq. (4). Indeed, such a substitution would alter the functional dependence of $\psi_\mathrm{i}[\cdot]$, $z + t$, thus violating the traveling-wave nature of the wave in vacuum!

4 Synthesis

This section deals with the synthesis problem, which consists in determining the trajectory of the moving interface required to achieve a desired pulse transformation. Specifically, we seek to solve Eq. (4) for $Z[t]$ as a function of the incident and reflected pulse envelopes, $\psi_{\mathrm{i}}[\cdot]$ and $\psi_{\mathrm{r}}[\cdot]$.

Solving Eq. (4) for the interface trajectory $Z[\cdot]$ is not straightforward. However, it turns out that the derivative of the argument of $\psi_{\mathrm{i}}[\cdot]$ in Eq. (4a) is its multiplicative factor, a fact that can be easily verified in the particular case of Eq. (5) and that drastically simplifies the problem. This allows to reformulate Eq. (4a) as a differential equation of the form (see Supplementary Sec. 2)

$$\psi_{\mathrm{r}}[x] = -\frac{d\xi}{dx}\psi_{\mathrm{i}}[\xi], \tag{6a}$$

where

$$\xi = \xi[x] = Z[f^{-1}[x]] - f^{-1}[x] \quad \text{and} \quad x = z + t. \tag{6b}$$

Grouping the terms in Eq. (6a) and integrating both sides, we obtain

$$\int \psi_{\mathrm{r}}[x]dx = -\int \psi_{\mathrm{i}}[\xi]d\xi. \tag{7}$$

This expression can be simplified by introducing the integral functions $F_{\mathrm{r}}[x] = \int \psi_{\mathrm{r}}[x]dx$ and $F_{\mathrm{i}}[\xi] = \int \psi_{\mathrm{i}}[\xi]d\xi$, leading to the compact relation

$$F_{\mathrm{i}}[\xi] = -F_{\mathrm{r}}[x]. \tag{8}$$

Solving this equation for ξ by applying $F_{\mathrm{i}}^{-1}[\cdot]$ to both sides and using Eq. (6b), we ultimately obtain the following explicit equation for the trajectory of the interface (see Supplementary Sec. 2):

$$Z[t] = \frac{1}{2}\left(L^{-1}[t] + F_{\mathrm{i}}^{-1}\left[-F_{\mathrm{r}}[L^{-1}[t]]\right]\right), \tag{9a}$$

where

$$L[t] = \frac{1}{2}\left(t - F_{\mathrm{i}}^{-1}\left[-F_{\mathrm{r}}[t]\right]\right). \tag{9b}$$

The calculation of $Z[t]$ using Eq. (9) must generally be performed numerically. However, an example admitting a closed-form result is provided in Supplementary Sec. 3 to better intuit the technique.

Rewriting Eq. (4a) locally in the form of Eq. (6a) and subsequently integrating both sides to obtain the global relation in Eq. (7) not only simplifies the mathematics to obtain the relation of Eq. (9), but also reveals a fundamental constraint on that equation: Eq. (7) indicates that the areas under the envelopes of $\psi_{\mathrm{i}}[\cdot]$ and $\psi_{\mathrm{r}}[\cdot]$ must be equal. This constraint can be intuitively understood by considering again the scattering relation for a uniformly moving PEC interface, given by Eq. (5). In this case, the Doppler shift factor $(1-v)/(1+v)$ stretches ($v > 0$) or compresses ($v < 0$) the phase of the pulse while inversely altering its amplitude so as to ensure global field conservation. This can be easily verified by inserting Eq. (5) into Eq. (7).

Thus, the desired reflected pulse, $\psi_{\mathrm{d}}[\cdot]$, must actually be scaled as

$$\psi_{\mathrm{r}} = \alpha\psi_{\mathrm{d}}, \tag{10a}$$

with the scaling factor

$$\alpha = -\frac{\int_{-\infty}^{+\infty}\psi_{\mathrm{i}}[\xi]d\xi}{\int_{-\infty}^{+\infty}\psi_{\mathrm{d}}[x]dx}, \tag{10b}$$

being generally different from minus one, $\alpha \neq -1$. In other words, if the desired pulse is not scaled as prescribed by Eq. (10), then it violates Eq. (7) and makes Eq. (9) invalid. Note that the *field* conservation in Eq. (7) does not mean that the *energy* is conserved at the interface. The energy is *not* conserved because of the breaking of temporal translational symmetry [46].

5 Examples

This section presents examples that demonstrate the effectiveness of our pulse shaping method. Given that Gaussian functions are among the most common occurrences of pulse envelopes, we focus on transforming a Gaussian-shaped pulse into various target waveforms.

Figure 2 demonstrates how a Gaussian pulse can be reshaped into a symmetric modulated Gaussian waveform with a different width, corresponding to the target envelope $E_{\mathrm{d}} = -\mathrm{e}^{-(\frac{0.7t}{\tau})^2}|\cos[20t]|$. Since the total integrals (i.e., area under the curve) of the incident pulse E_{i} and desired pulse E_{d} are not equal, we first rescale E_{d} to obtain the physically realizable reflected pulse E_{r}, as depicted in Fig. 2(a). This ensures field conservation, following the rescaling relation in Eq. (10b). The required trajectory of the moving interface to transform E_{i} into E_{r} is then numerically computed using Eq. (9). The resulting scattering is shown in Fig. 2(b). Interestingly, the interface follows a predominantly forward-moving trajectory with superimposed oscillations. This can be intuitively understood as a combination of two key components: a uniform velocity motion that stretches the pulse base (corresponding to the $0.7/\tau$ term) and an oscillatory motion that introduces the modulation (corresponding to the $\cos[20t]$ term). To provide a clearer understanding of the pulse evolution, Fig. 2(c) presents discrete temporal snapshots from Fig. 2(b), illustrating how the incident Gaussian pulse progressively morphs into the modulated Gaussian shape as it interacts with the moving PEC interface.

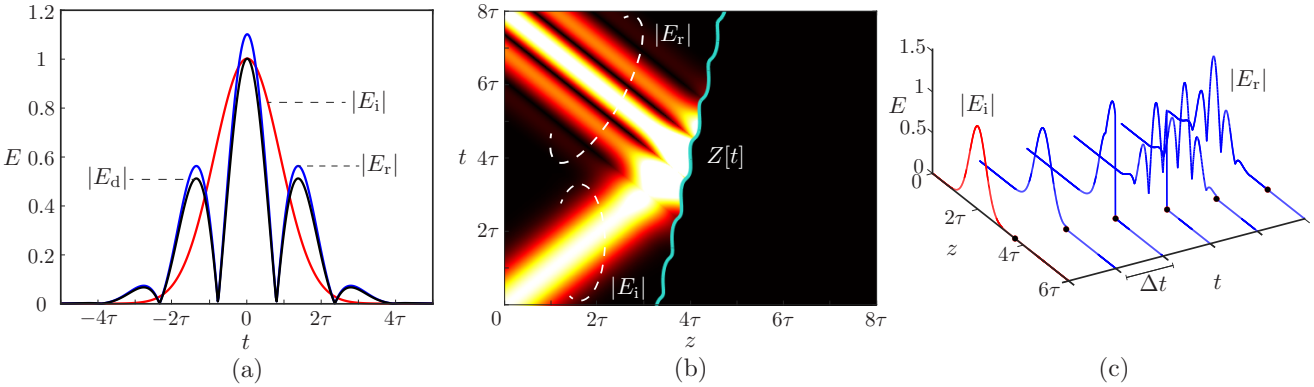

Figure 2: Shaping a Gaussian envelope, given by $E_{\mathrm{i}} = \mathrm{e}^{-(\frac{t}{\tau})^2}$, into $E_{\mathrm{d}} = -\mathrm{e}^{-(\frac{0.7t}{\tau})^2}|\cos[20t]|$. (a) Incident, desired and reflected pulses in the retarded frame. (b) Space-time representation of the interface trajectory and pulse shaping. (c) Discrete snapshots from (b) showing the evolution of the pulse.

Figure 3 presents another example of pulse shaping, where a Gaussian pulse is transformed into a smooth rectangular waveform, defined as $E_{\mathrm{d}} = -\frac{1}{2}(\tanh[-30t+10] - \tanh[-30t-10])$. The rescaled version of the target pulse, E_{r}, is shown in Fig. 3(a). Here, the rescaling mismatch between the incident field and the target field is even more apparent than in the previous example. The space-time evolution of the pulse, along with the computed trajectory of the interface, is displayed in Fig. 3(b). Notably, the interface exhibits sudden velocity changes at both the leading and trailing edges of the pulse. This behavior can be understood by considering the necessary transformations: the interface must sharply amplify the leading edge of the Gaussian pulse to create the steep rise of the rectangular waveform. To achieve this, the interface moves rapidly toward the pulse, inducing a strong Doppler compression. Subsequently, the interface recedes to attenuate and smooth the central portion of the pulse. Finally, it rapidly advances again to carve the sharp trailing edge. As in the previous case, Fig. 3(c) provides discrete snapshots illustrating the progressive evolution of the pulse as it interacts with the moving interface.

Pulse shaping is not limited to simple, symmetric transformations. Figure 4 demonstrates how a Gaussian pulse can be reshaped into a more intricate, multi-peaked waveform resembling the camel-shaped envelope depicted in Fig. 1. The target pulse is defined as $E_{\mathrm{d}} = -\mathrm{e}^{-(\frac{2t}{\tau})^2} - \mathrm{e}^{-(\frac{2(t-0.1)}{\tau})^2} - 1.5\mathrm{e}^{-(\frac{t+0.1}{\tau})^2}\mathrm{e}^{-(\frac{t+0.2}{\tau})^2}$. As in the previous examples, field conservation requires the target pulse to be rescaled, yielding E_{r}, which is shown in Fig. 4(a). Using Eq. (9), we compute the required trajectory of the PEC interface, and the resulting space-time evolution is illustrated in Fig. 4(b). To achieve such a complex transformation, the interface must perform a sequence of precise back-and-forth oscillations. Each abrupt forward motion generates a peak in the reflected wave, while each retreating motion suppresses a portion of the pulse, forming valleys between the peaks. This subtle interplay of compressive and expansive Doppler shifts effectively sculpts the incident Gaussian into the desired multi-peaked waveform. As before, Fig. 4(c) provides discrete snapshots, visually capturing the gradual evolution of the pulse as it interacts with the moving interface.

To globally validate the proposed pulse shaping method, we finally perform a finite-difference time-domain (FDTD) simulation using a generalized Yee grid [43] that ensures that the moving boundary conditions at the interface, as described by Eq. (2), are properly satisfied. The simulation results are presented in Fig. 5. In this case, we reshape a single Gaussian pulse into two separate Gaussian pulses of different widths, defined as $E_{\mathrm{r}} = -2.4\mathrm{e}^{(-\frac{t-1.32}{0.1\tau})^2} - 2.4\mathrm{e}^{(-\frac{t+1.32}{0.1\tau})^2}$.

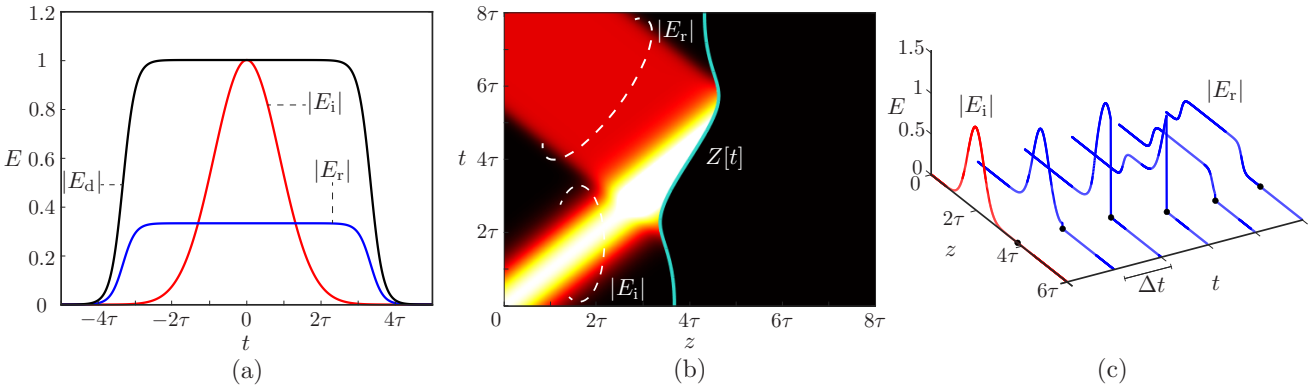

Figure 3: Shaping a Gaussian envelope, given by $E_{\mathrm{i}} = \mathrm{e}^{-(\frac{t}{\tau})^2}$, into a smooth rectangular pulse given by $E_{\mathrm{d}} = -\frac{1}{2}(\tanh[-30t+10] - \tanh[-30t-10])$. (a) Incident, desired and reflected pulses in the retarded frame. (b) Space-time representation of the envelope shaping. (c) Discrete snapshots from (b) showing the evolution of the pulse.

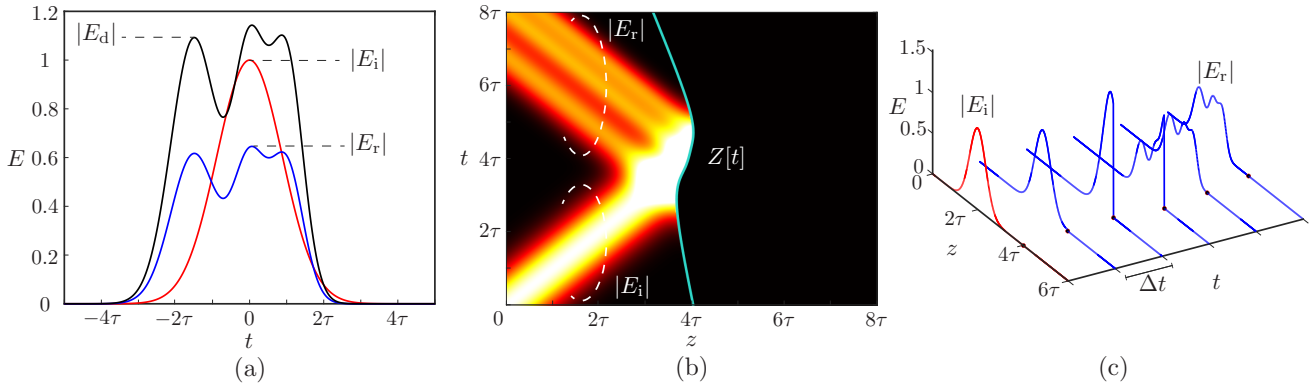

Figure 4: Shaping a Gaussian envelope, given by $E_{\mathrm{i}} = \mathrm{e}^{-(\frac{t}{\tau})^2}$, into $E_{\mathrm{d}} = -\mathrm{e}^{-(\frac{2t}{\tau})^2} - \mathrm{e}^{-(\frac{2(t-0.1)}{\tau})^2} - 1.5\mathrm{e}^{-(\frac{t+0.1}{\tau})^2}\mathrm{e}^{-(\frac{t+0.2}{\tau})^2}$. (a) Incident, desired and reflected pulses in the retarded frame. (b) Space-time representation of the envelope shaping. (c) Discrete snapshots from (b) showing the evolution of the pulse.

Figure 5(a) compares the analytical results obtained from Eq. (9) with those numerically obtained by FDTD. A relatively good agreement is observed, except for some discrepancy due to instability of the scheme when the velocity approaches the speed of light [43], confirming the accuracy of our theoretical predictions. The space-time evolution of the scattering process, along with the corresponding interface trajectory, is depicted in Fig. 5(b). The shaping mechanism follows a well-defined sequence: the interface initially moves backward with high velocity to create the leading Gaussian peak, then rapidly retreats at a velocity close to the speed of light to introduce the separation between the two peaks, and finally advances again to generate the second Gaussian peak. Figure 5(c) presents the usual discrete temporal snapshots.

Note that although breaking temporal translational symmetry, the nonuniform interfaces considered in this paper, involving no external force [47], do *not* break time-reversal symmetry [48, 49]. This means that a reflected pulse can be transformed back into its original shape by scattering off an interface that follows a time-reversed trajectory. In other words, if a pulse is shaped into a desired waveform using a specific interface motion, an interface moving in the exact opposite manner restores it to its original form. This property can be intuitively understood by considering the uniform motion case described by Eq. (5). Suppose a wave undergoes scattering at a uniformly moving PEC interface, as illustrated in Fig. 1(a). According to Eq. (5), the scattered wave experiences a Doppler shift with an amplitude scaling factor of $(1-|v|)/(1+|v|)$. where v is the normalized velocity of the interface. Now, if this scattered wave subsequently interacts with an interface moving in the opposite direction ($v \to -v$), as shown in Fig. 1(b), it experiences the inverse Doppler shift with a scaling factor of $(1+|v|)/(1-|v|)$. This exact reversal cancels out the previous transformation, restoring the pulse to its original form.

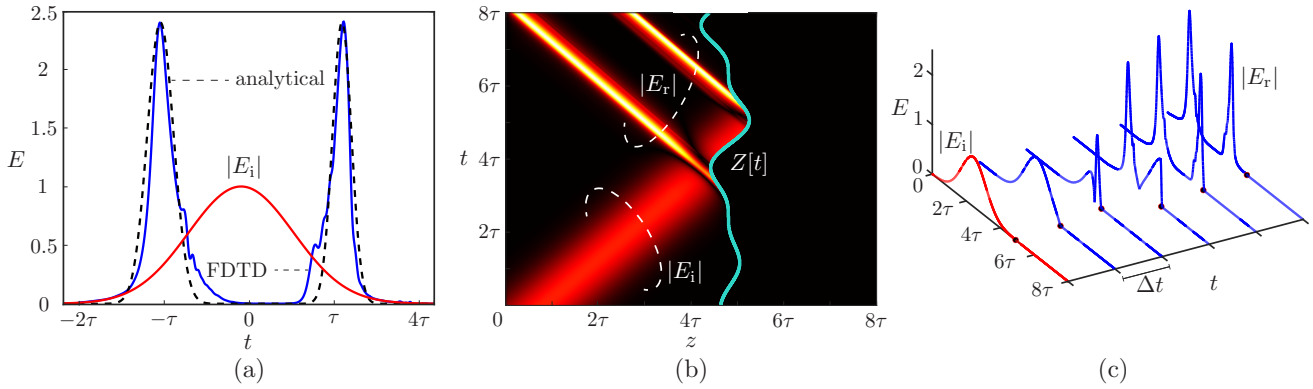

Figure 5: FDTD validation of pulse shaping a Gaussian, given by $E_i = e^{-(\frac{t}{\tau})^2}$, into $E_r = -2.4e^{(-\frac{t-1.32}{0.1\tau})^2} - 2.4e^{(-\frac{t+1.32}{0.1\tau})^2}$. (a) Incident (red), analytical reflection (dashed black) and FDTD (blue). (b) Space-time representation of the pulse shaping. Discrete snapshots from (b) showing the evolution of the pulse.

6 Conclusion

In this work, we introduced a novel pulse shaping method based on nonuniform Doppler shifts induced by an accelerated PEC interface. By leveraging the motion of the interface, we demonstrated how an incident pulse can be precisely transformed into a desired waveform without relying on spectral filtering or nonlinear effects. We established an analytical closed-form relation for scattering at an arbitrarily moving PEC interface. We formulated the inverse problem to determine the required trajectory that reshapes an input pulse into a specified target waveform. To illustrate the versatility of this approach, we applied it to a series of examples, transforming Gaussian pulses into symmetric modulated, rectangular and complex multi-peaked waveforms. The results revealed how different interface motion profiles—ranging from uniform velocity to oscillatory and abrupt movements—enable precise envelope manipulation. Additionally, we validated our theoretical framework through FDTD simulations. The proposed technique opens new possibilities for ultrafast optics, optical signal processing and waveform synthesis. Compared to conventional pulse shaping methods, it provides a physically intuitive and dynamically tunable approach to modifying pulse envelopes. Future research could explore experimental realizations of this concept and extensions to more complex media, such penetrable and dispersive interfaces. Furthermore, potential applications in optical computing, quantum information processing and analog signal transformation could be investigated.

References

[1] Bahaa EA Saleh and Malvin Carl Teich. *Fundamentals of Photonics*. John Wiley & Sons, 2019.

[2] Donna Strickland and Gerard Mourou. Compression of amplified chirped optical pulses. *Opt. Commun.*, 55(6):447–449, 1985.

[3] BE Lemoff and CPJ Barty. Quintic-phase-limited, spatially uniform expansion and recompression of ultrashort optical pulses. *Opt. lett.*, 18(19):1651–1653, 1993.

[4] Andrew M Weiner, Yaron Silberberg, Henning Fouckhardt, Daniel E Leaird, MA Saifi, MJ Andrejco, and Peter W Smith. Use of femtosecond square pulses to avoid pulse breakup in all-optical switching. *IEEE J. Quantum Electron.*, 25(12):2648–2655, 1989.

[5] Andreas Assion, T Baumert, M Bergt, T Brixner, B Kiefer, V Seyfried, M Strehle, and G Gerber. Control of chemical reactions by feedback-optimized phase-shaped femtosecond laser pulses. *Science*, 282(5390):919–922, 1998.

[6] H Shi, J Finlay, GA Alphonse, JC Connolly, and PJ Delfyett. Multiwavelength 10-ghz picosecond pulse generation from a single-stripe semiconductor diode laser. *IEEE Photonics Technol. Lett.*, 9(11):1439–1441, 1997.

[7] Sterling Backus, Charles G Durfee III, Margaret M Murnane, and Henry C Kapteyn. High power ultrafast lasers. *Rev. Sci. Instrum.*, 69(3):1207–1223, 1998.

[8] M Ulman, DW Bailey, LH Acioli, FG Vallee, CJ Stanton, EP Ippen, and JG Fujimoto. Femtosecond tunable nonlinear absorption spectroscopy in Al 0.1 Ga 0.9 As. *Phys. Rev. B*, 47(16):10267, 1993.

[9] Constantin Brif, Raj Chakrabarti, and Herschel Rabitz. Control of quantum phenomena: Past, present and future. *New J. Phys.*, 12(7):075008, 2010.

[10] Christophe Caloz, Shulabh Gupta, Qingfeng Zhang, and Babak Nikfal. Analog signal processing: A possible alternative or complement to dominantly digital radio schemes. *IEEE Microw. Mag.*, 14(6):87–103, 2013.

[11] Jens Thomas, Christian Voigtlaender, Ria G Becker, Daniel Richter, Andreas Tuennermann, and Stefan Nolte. Femtosecond pulse written fiber gratings: A new avenue to integrated fiber technology, 2012.

[12] Roberto Osellame, Giulio Cerullo, and Roberta Ramponi. *Femtosecond laser micromachining: Photonic and microfluidic devices in transparent materials*, volume 123. Springer Science & Business Media, 2012.

[13] Warren S Warren, Herschel Rabitz, and Mohammed Dahleh. Coherent control of quantum dynamics: The dream is alive. *Science*, 259(5101):1581–1589, 1993.

[14] Andrew M Weiner. Ultrafast optical pulse shaping: A tutorial review. *Opt. Commun.*, 284(15):3669–3692, 2011.

[15] ME Fermann, V Da Silva, DA Smith, Y Silberberg, and AM Weiner. Shaping of ultrashort optical pulses by using an integrated acousto-optic tunable filter. *Opt. lett.*, 18(18):1505–1507, 1993.

[16] AM Weiner DE Leaird, Jay S Patel, and JR Wullert. Programmable femtosecond pulse shaping by use of a multielement liquid-crystal phase modulator. *Opt. Lett*, 15:326, 1990.

[17] KF Kwong, D Yankelevich, KC Chu, JP Heritage, and A Dienes. 400-hz mechanical scanning optical delay line. *Opt. Lett.*, 18(7):558–560, 1993.

[18] JP Heritage, EW Chase, RN Thurston, and M Stern. A simple femtosecond optical third-order disperser. In *Conference on Lasers and Electro-optics*, page CTuB3. Optica Publishing Group, 1991.

[19] Sven Breitkopf, Tino Eidam, Arno Klenke, Lorenz Von Grafenstein, Henning Carstens, Simon Holzberger, Ernst Fill, Thomas Schreiber, Ferenc Krausz, Andreas Tünnermann, et al. A concept for multiterawatt fibre lasers based on coherent pulse stacking in passive cavities. *Light Sci. Appl.*, 3(10):e211–e211, 2014.

[20] Andrew M Weiner. Femtosecond pulse shaping using spatial light modulators. *Rev. Sci. Instrum.*, 71(5):1929–1960, 2000.

[21] Curt W Hillegas, Jerry X Tull, Debabrata Goswami, Donna Strickland, and Warren S Warren. Femtosecond laser pulse shaping by use of microsecond radio-frequency pulses. *Opt. Lett.*, 19(10):737–739, 1994.

[22] MA Dugan, JX Tull, and WS Warren. High-resolution acousto-optic shaping of unamplified and amplified femtosecond laser pulses. *JOSA B*, 14(9):2348–2358, 1997.

[23] Christophe Caloz, Zoé-Lise Deck-Léger, Amir Bahrami, Oscar Céspedes Vicente, and Zhiyu Li. Generalized space-time engineered modulation (GSTEM) metamaterials: A global and extended perspective. *IEEE Antennas Propag. Mag.*, 65(4):50–60, 2023.

[24] Edwards S Cassedy and Arthur A Oliner. Dispersion relations in time-space periodic media: Part I—Stable interactions. *Proc. IEEE*, 51(10):1342–1359, 1963.

[25] Edwards S Cassedy. Dispersion relations in time-space periodic media: Part II—Unstable interactions. *Proc. IEEE*, 55(7):1154–1168, 1967.

[26] William T Rhodes. Acousto-optic signal processing: Convolution and correlation. *Proc. IEEE*, 69(1):65–79, 1981.

[27] A. M. Shaltout, V. M. Shalaev, and M. L. Brongersma. Spatiotemporal light control with active metasurfaces. *Science*, 364(6441):1–10, May 2019.

[28] A. Fresnel. Lettre d'Augustin Fresnel à François Arago sur l'influence du mouvement terrestre dans quelques phénomènes d'optiques. *Ann. Chim. Phys*, 9:57–66, 1818.

[29] Hippolyte Fizeau. Sur les hypothèses relatives à l'éther lumineux, et sur une expérience qui parait démontrer que le mouvement des corps change la vitesse avec laquelle la lumière se propage dans leur intérieur. *CR Acad. Sci.*, 33:349–355, 1851.

[30] Christian Doppler. Über das farbige Licht der Doppelsterne und einiger anderer Gestirne des Himmels. *Königl. Böhm Gedsellsch. d. Wis.*, 2:465–482, 1842.

[31] C. Yeh. Reflection and transmission of electrodynamic waves by a moving dielectric medium. *J. Appl. Phys.*, 36(11):3513–3516, 1965.

[32] Paloma A Huidobro, Emanuele Galiffi, Sébastien Guenneau, Richard V Craster, and J. B. Pendry. Fresnel drag in space–time-modulated metamaterials. *Proc. Natl. Acad. Sci.*, 116(50):24943–24948, 2019.

[33] Daniele Faccio, Francesco Belgiorno, Sergio Cacciatori, Vittorio Gorini, Stefano Liberati, and Ugo Moschella. *Analogue Gravity Phenomenology: Analogue Spacetimes and Horizons, from Theory to Experiment*, volume 870. Springer, 2013.

[34] Daniele Faccio, Tal Arane, Marco Lamperti, and Ulf Leonhardt. Optical black hole lasers. *Class. Quantum Grav.*, 29(22):224009, 2012.

[35] F. R. Morgenthaler. Velocity modulation of electromagnetic waves. *IRE Trans. Microw. Theory Tech.*, 6(2):167–172, Apr. 1958.

[36] Christophe Caloz and Zoé-Lise Deck-Léger. Spacetime metamaterials—Part I: General concepts. *IEEE Trans. Antennas Propag.*, 68(3):1569–1582, 2019.

[37] E Galiffi, MG Silveirinha, PA Huidobro, and JB Pendry. Photon localization and Bloch symmetry breaking in luminal gratings. *Phys. Rev. B*, 104(1):014302, 2021.

[38] Zoé-Lise Deck-Léger, Nima Chamanara, Maksim Skorobogatiy, Mário G Silveirinha, and Christophe Caloz. Uniform-velocity spacetime crystals. *Adv. Photonics*, 1(5):056002, 2019.

[39] Tie Jun Cui, Shuang Zhang, Andrea Alù, Martin Wegener, Sir John Pendry, Jie Luo, Yun Lai, Zuojia Wang, Xiao Lin, Hongsheng Chen, Ping Chen, Rui-Xin Wu, Yuhang Yin, Pengfei Zhao, Huanyang Chen, Yue Li, Ziheng Zhou, Nader Engheta, Viktar Asadchy, Constantin Simovski, Sergei Tretyakov, Biao Yang, Sawyer D Campbell, Yang Hao, Douglas H Werner, Shulin Sun, Lei Zhou, Su Xu, Hong-Bo Sun, Zhou Zhou, Zile Li, Guoxing Zheng, Xianzhong Chen, Tao Li, Shining Zhu, Junxiao Zhou, Junxiang Zhao, Zhaowei Liu, Yuchao Zhang, Qiming Zhang, Min Gu, Shumin Xiao, Yongmin Liu, Xianzhe Zhang, Yutao Tang, Guixin Li, Thomas Zentgraf, Kirill Koshelev, Yuri Kivshar, Xin Li, Trevon Badloe, Lingling Huang, Junsuk Rho, Shuming Wang, Din Ping Tsai, A Yu Bykov, A V Krasavin, A V Zayats, Cormac McDonnell, Tal Ellenbogen, Xiangang Luo, Mingbo Pu, Francisco J Garcia-Vidal, Liangliang Liu, Zhuo Li, Wenxuan Tang, Hui Feng Ma, Jingjing Zhang, Yu Luo, Xuanru Zhang, Hao Chi Zhang, Pei Hang He, Le Peng Zhang, Xiang Wan, Haotian Wu, Shuo Liu, Wei Xiang Jiang, Xin Ge Zhang, Cheng-Wei Qiu, Qian Ma, Che Liu, Long Li, Jiaqi Han, Lianlin Li, Michele Cotrufo, C Caloz, Z-L Deck-Léger, A Bahrami, O Céspedes, E Galiffi, P A Huidobro, Qiang Cheng, Jun Yan Dai, Jun Cheng Ke, Lei Zhang, Vincenzo Galdi, and Marco di Renzo. Roadmap on electromagnetic metamaterials and metasurfaces. *J. Phys. Photonics*, 6(3):032502, 2024.

[40] Jamison Sloan, Nicholas Rivera, John D Joannopoulos, and Marin Soljačić. Controlling two-photon emission from superluminal and accelerating index perturbations. *Nat. Phys.*, 18(1):67–74, 2022.

[41] Amir Bahrami, Zoé-Lise Deck-Léger, and Christophe Caloz. Electrodynamics of accelerated-modulation space-time metamaterials. *Phys. Rev. Appl.*, 19(5):054044, 2023.

[42] Amir Bahrami, Klaas De Kinder, Zhiyu Li, and Christophe Caloz. Space-time wedges. *Nanophotonics*, 2025.

[43] Amir Bahrami, Zoé-Lise Deck-Léger, Zhiyu Li, and Christophe Caloz. A generalized FDTD scheme for moving electromagnetic structures with arbitrary space-time configurations. *IEEE Trans. Antennas Propag.*, 72(2):1721–1734, 2024.

[44] Klaas De Kinder and Christophe Caloz. Electromagnetic scattering at an arbitrarily accelerated interface. In *Metamaterials*, pages 1–3, 2024.

[45] J Cooper. The scattered field from a moving flat plate: The one dimensional case. *IEEE Trans. Antennas Propag.*, 28(6):791–795, 1980.

[46] Zhiyu Li, Xikui Ma, Zoé-Lise Deck-Léger, Amir Bahrami, and Christophe Caloz. Wave-medium interactions in dynamic matter and modulation systems. *IEEE Trans. Antennas Propag.*, 2025.

[47] Christophe Caloz, Andrea Alu, Sergei Tretyakov, Dimitrios Sounas, Karim Achouri, and Zoé-Lise Deck-Léger. Electromagnetic nonreciprocity. *Phys. Rev. Appl.*, 10(4):047001, 2018.

[48] Vincent Bacot, Matthieu Labousse, Antonin Eddi, Mathias Fink, and Emmanuel Fort. Time reversal and holography with spacetime transformations. *Nat. Phys.*, 12(10):972–977, 2016.

[49] Z.-L. Deck-Léger, A. Akbarzadeh, and C. Caloz. Wave deflection and shifted refocusing in a medium modulated by a superluminal rectangular pulse. *Phys. Rev. B*, 97(10):104305–1:7, Mar. 2018.